Global Health & Medicine. 2024; 6(4):236-243.
ORIGINAL ARTICLE
DOI: 10.35772/ghm.2024.01037

Effects of low-frequency ultrasound combined with microbubbles on breast cancer xenografts in nude mice

Xiaoli Peng[1,§], Lisha Li[2,3,4,§], Yingchun Liu[1], Yuqing Guo[1], Yun Pang[1], Shengnan Ding[1], Jing Zhou[2,3,4], Ling Wang[2,3,4,*], Lin Chen[1,*]

[1] Department of Ultrasound, Huadong Hospital, Fudan University, Shanghai, China;
[2] Laboratory for Reproductive Immunology, Obstetrics and Gynecology Hospital of Fudan University, Shanghai, China;
[3] The Academy of Integrative Medicine of Fudan University, Shanghai, China;
[4] Shanghai Key Laboratory of Female Reproductive Endocrine-related Diseases, Shanghai, China.

Abstract: The aim of this study was to explore the effects of low-frequency ultrasound (US) combined with microbubbles (MBs) on breast cancer xenografts and explain its underlying mechanisms. A total of 20 xenografted nude mice were randomly divided into four groups: a group treated with US plus MBs (the US + MBs group), a group treated with US alone (the US group), a group treated with MBs alone (the MBs group), and a control group. In different groups, mice were treated with different US and injection regimens on an alternate day, three times in total. Histological changes, apoptosis of cells, microvascular changes, and the apoptosis index (AI) and microvascular density (MVD) of the breast cancer xenograft were analyzed after the mice were sacrificed. Results indicated that the tumor volume in the US + MBs group was smaller than that in the other three groups ($p < 0.001$ for all). The rate of tumor growth inhibition in the US + MBs group was significantly higher than that in the US and MBs groups ($p < 0.001$ for both). There were no significant differences in histological changes among the four groups. However, the AI was higher in the US + MBs group than that in the other three groups while the MVD was lower ($p < 0.001$ for all). All in all, low-frequency US combined with MBs can effectively slow down the growth of breast cancer in nude mice. In summary, low-frequency US combined with MBs has a significant effect on breast cancer treatment. Cavitation, thermal effects, and mechanical effects all play a vital role in the inhibition of tumor growth.

***Keywords*:** low-frequency ultrasound irradiation treatment, nude mouse xenograft model of breast cancer, ultrasonic cavitation

Introduction

Worldwide, female breast cancer was the most common cancer with around 2.3 million new cases (11.7%) and the fifth leading cause of cancer death with around 0.7 million new deaths (*1*). Although more new cases were diagnosed in women over the age of 50, its incidence in younger women is rising (*2*). In China, breast cancer was the most common cause of cancer death (16.7%) in women ages 15-44 (*3*). Screening technology is becoming more mature and widespread, and more breast cancers of a smaller volume are detected at an even earlier stage (*4*). Therefore, early diagnosis and appropriate treatment affect patient prognosis. With the spread of breast-conserving surgery and the widespread use of pre- and postoperative adjuvant therapy, local treatment of breast cancer is developing rapidly (*5*). According to different tumor types and stages, different local treatments can be selected, such as radiotherapy (*6*), radiofrequency ablation (*7*), and microwave ablation (*8*).

Ultrasound (US) is now one of the hot fields in treating solid tumors. Bioeffects of US mainly consist of thermal effects, cavitation, and mechanical effects. High-intensity focused ultrasound (HIFU), as a therapy with thermal effects, has been used clinically to treat various solid tumors, like liver cancer and thyroid cancer (*9,10*). However, HIFU is still not widely used in breast cancer due to technical and equipment limitations, and it has a variety of complications, such as pain, skin burns, edema of the lungs, and major pectoralis injury. As a non-thermal therapy, low-frequency US has been widely studied in promoting cell apoptosis *in vitro* and *in vivo* (*11-14*). Cavitation plays an essential role in the inhibition of tumor growth by low-frequency US. According to the state of MB motion, cavitation is divided into stable cavitation and inertial cavitation; in the former, MBs move in

periodic, nonlinear oscillations under the action of periodically varying US. In the latter, MBs periodically expand and contract until they burst, releasing large amounts of energy. Low-frequency US has not been studied in depth in terms of its efficacy and mechanism of action in breast cancer. In our previous work, we found that the most suitable exposure parameters were a frequency of 1 MHz, an intensity of 2 W/cm^2, a duty cycle of 50%, and an exposure time of 5 min. The aim of the current study was to explore the effects of low-frequency US combined with MBs and explain its underlying mechanisms.

Materials and Methods

Cell culture

MDA-MB-231 cells (Shanghai Cancer Institute) were cultured in a RPMI-1640 medium (Gibco, America) supplemented with 10% of FBS (HyClone, US) at 37°C in an atmosphere of humidified 5% CO2. All experiments were performed in accordance with the requirements of the Guidelines for the Care and Use of Laboratory Animals and were approved by the Animal Experiment Ethics Committee of Shanghai Medical College of Fudan University.

Xenograft model establishment and sample collection

Female Balb/c nude mice (4-5 weeks old, 18-24 g) were acquired from Shanghai Xipur-Bikai Experimental Animal Co. Mice were bred under special pathogen-free (SPF) conditions.

When MDA-MB-231 cells reached the logarithmic phase, they were digested with a 0.25% EDTA trypsin digestive solution (Gibco, America), suspended, and harvested by centrifugation at 1,200 rpm for 5 min. A total of 1×10^6 cells suspended in 100 μL of PBS were injected subcutaneously under the second pair of right mammary fat pads of each nude mouse. After injection, the tumor growth was observed, and on the 10th day, the tumor grew to 10 mm, and the xenograft model was successfully established.

US treatment procedures

The US750 low-frequency ultrasonic therapeutic instrument (ITO Co. Ltd., Japan) was used in this study. US exposure was as follows: a frequency of 1 MHz, an intensity of 2 W/cm^2, a duty cycle of 50%, and exposure time of 5 min. SonoVue (Bracco, Milan, Italy), which contained sulfur hexafluoride gas and had a phospholipid monolayer shell, was shaken with 5 mL of normal saline into a MB suspension, and 0.2 mL of the MB suspension was injected into the mouse via the tail vein.

A total of 20 xenografted nude mice were randomly divided into four groups. The US plus MBs (US + MBs) group was treated with MBs followed by US. The MBs group was treated with MBs combined with empty exposure. The US group was treated with saline followed by US. The control group was treated with saline combined with empty exposure. All of the mice had undergone US or empty irradiation on an alternate day, three times in total. After the third treatment, all mice were kept under SPF conditions for 6 days. Afterwards, all xenografted mice were sacrificed. The tumors were removed for observation and fixed in formalin for further study.

Measurement of tumor growth

The tumor volume was calculated with the following formula: Volume (V) = $(\pi \times a \times b^2)/6$. The length (a) and width (b) of tumors were measured before each irradiation and every other day after the last irradiation, six times in total. The following formula was used to calculate the rate of tumor growth inhibition (TGI): TGI (%) = $(1 - V/V_0) \times 100\%$. (V represented the final volume in treatment groups, and V_0 represented the final volume in the control group)

Hematoxylin and eosin (H&E) staining

The harvested tumor specimens were fixed in a 4% formalin solution for 24 h. The tissues were embedded in paraffin and then cut into 4-μm-thick sections. The sections were stained with H&E for pathological examination. A microscope was used to photograph the sections at ×400 magnification to observe the tumor tissue pathology and structural changes.

Terminal deoxynucleotidyl transferase dUTP nick-end labeling (TUNEL) assay

Using the In Situ Cell Death Detection Kit (POD, Roche company, Germany), apoptosis of the tumor cells was determined with TUNEL. Apoptotic cells with DNA fragmentation stained brown. Slides were counterstained with hematoxylin, and the apoptotic cells stained brownish-yellow. The total number of tumor cell nuclei and TUNEL-positive cell nuclei were counted (magnification, ×400). Eight high-magnification fields were analyzed in each section. The positive cells and total cells in every field were counted and then the apoptosis index (AI) was calculated using the following formula: AI = (Number of positive cells/Number of whole cells) × 100%. The AI of all eight fields was averaged as the AI for the section.

CD34 immunohistochemical staining

The paraffin sections were dewaxed. The tissue sections were incubated with 3% methanol hydrogen peroxide for 5 min at room temperature, washed with PBS

three times to block endogenous peroxidases, and then blocked with dilute goat serum at room temperature for 20 min to block nonspecific antigens. Then, the tissues were continuously incubated with CD34 antibodies overnight, secondary antibodies for 20 min, and the chromogenic agent for 20 min, followed by hematoxylin counterstaining, dehydration, and mounting. The nuclei and cytoplasm of vascular endothelial cells stained brownish-yellow. The sections were observed under 40× magnification to determine areas of high blood vessel density, *i.e.*, hot spots. The number of vessels in hot spots was counted under 400× magnification. After observing five hot spots, the microvascular density (MVD) was calculated.

Statistics

Quantitative data are expressed as the mean ± standard deviation. Differences between or within groups were tested using one-way analysis of variance (ANOVA), and differences in ratios were tested using a chi-squared test. A *P* value<0.05 indicated statistical significance, and a *p* value<0.001 indicated marked statistical significance. Statistical analysis was performed using the software SPSS 13.0.

Results

Low-frequency US combined with MBs inhibited tumor growth

Tumor growth was significantly inhibited in the US + MBs group. The tumor volume in the US+MBs group (0.961 ± 0.490 mm^3, $p < 0.001$) was smaller than that in the control (2.067 ± 0.281 mm^3, $p < 0.001$), MBs (1.949 ± 0.250 mm^3, $p < 0.001$), and US groups (1.542 ± 0.133 mm^3, $p < 0.001$), and the TGI in the US + MBs group (53.51%, $p < 0.001$) was greater than that in the MBs (10.98%, $p < 0.001$) and US groups (25.40%, $p < 0.001$). Compared to the control and MBs groups, the tumor volume in the US group was markedly smaller ($p < 0.05$ for both), and the TGI in the US group was higher than that in the MBs group ($p < 0.001$). There were no significant differences in the tumor volume in the control and MBs groups ($p > 0.05$). The trends in tumor growth in the four groups are shown in Figure 1. Tumor volumes and TGIs are shown in Table 1.

Low-frequency US combined with MBs reduced erythrocyte-filled vessels without other pathological changes

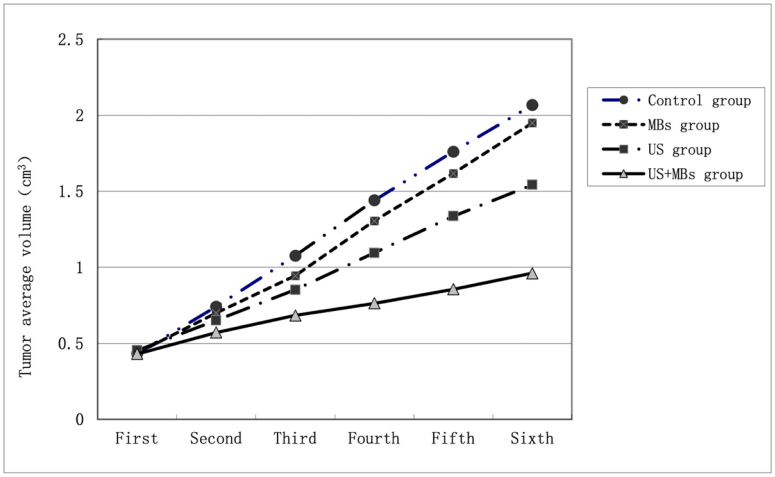

Figure 1. Growth trends for breast cancer xenografts. Tumor growth in the US + MBs group slowed down significantly and the slope was relatively slight. Tumor growth in the US group slowed down, and the slope was steeper than that in the US + MBs group. Trends in tumor growth were similar in the MBs and control groups, and the slopes were steep.

Table 1. Comparison of tumor growth in each group after treatment

Group	*n*	Tumor volume before treatment (mm^3)	Tumor volume before execution (mm^3)	TGI (%)
Control	5	0.434 ± 0.065	2.067 ± 0.281	-
MBs	5	0.437 ± 0.062	1.949 ± 0.250	10.98
US	5	0.454 ± 0.062	1.542 ± 0.133[a]	25.40[c]
US + MBs	5	0.431 ± 0.025	0.961 ± 0.490[b]	53.51[d]

(a) $p < 0.05$, US *vs*. Control, MBs, respectively; $p < 0.001$, US *vs.* US + MBs. (b) $p < 0.001$, US + MBs *vs.* Control, MBs, US, respectively. (c) $p < 0.001$, US *vs*. MBs. (d) $p < 0.001$, US + MBs *vs.* MBs, US, respectively. US: ultrasound; MBs: microbubbles; TGI: rate of tumor growth inhibition.

Pathological changes in tumor tissues are shown in Figure 2. H&E staining did not reveal noticeable histological differences in each group, and no apparent necrosis was observed. Under microscopic observation, the number of erythrocyte-filled vessels decreased in the US + MBs group compared to the other three groups. Erythrocyte leakage was seen in the interstitium in some areas in the US + MBs group.

Low-frequency US combined with MBs increased apoptosis

As shown in the TUNEL assay, the distribution of apoptotic cells in each group are shown in Figure 3. A few scattered stained apoptotic cells were seen in the control and MBs groups. In the US group, the number of apoptotic cells increased, and they were scattered. In the US + MBs group, apoptotic cells increased significantly, and they were present in sheets, and especially around blood vessels. The AI in the US + MBs group (49.02 ± 2.85%) was significantly higher than that in the other three groups (US: 11.04 ± 0.34%; MBs: 6.15 ± 0.29%; control: 4.68 ± 0.22%; $p < 0.001$ for all). The AI in the US group was markedly higher than that in the control and MBs groups ($p < 0.001$ for both). There were no significant differences in the AI in the MBs and control groups ($p > 0.05$). The AIs in the four group are shown in Table 2.

Low-frequency US combined with MBs reduced the microvascular density

After CD34 staining, the microvascular endothelium stained brownish-yellow, as shown in Figure 4. In the control and MBs groups, several microvessels were observed in areas where the tumor thrived. However, the number of microvessels decreased in the US group. In the US + MBs group, the number of microvessels decreased significantly, and the residual lumens were

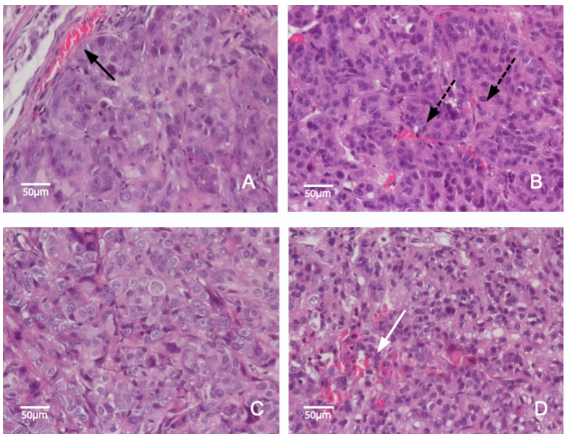

Figure 2. H&E staining of breast cancer xenografts (×400). (A) In the control group, donor blood vessels are visible at the edge of the tumor, and the lumen is filled with erythrocytes (black arrow). **(B)** In the MBs group, a few vessels are seen in the tumor, and a few erythrocytes are seen in the lumen (dotted arrow). **(C)** There are few vessels in the US group. **(D)** In the US + MBs group, erythrocytes leaked into the interstitium (white arrow). H&E: hematoxylin and eosin.

Table 2. Comparison of AI and MVD after treatment among groups

Group	*n*	AI (%)	MVD
Control	5	4.68 ± 0.22	10.93 ± 0.37
MBs	5	6.15 ± 0.29	10.48 ± 0.44
US	5	11.04 ± 0.34[a]	6.59 ± 0.24[a]
US + MBs	5	49.02 ± 2.85[b]	3.75 ± 0.36[b]

(a) $p < 0.001$, US *vs.* Control, MBs, US + MBs, respectively. (b) $p < 0.001$, US + MBs *vs.* Control, MBs, US, respectively. MVD: microvascular density; AI: apoptosis index; US: ultrasound; MBs: microbubbles.

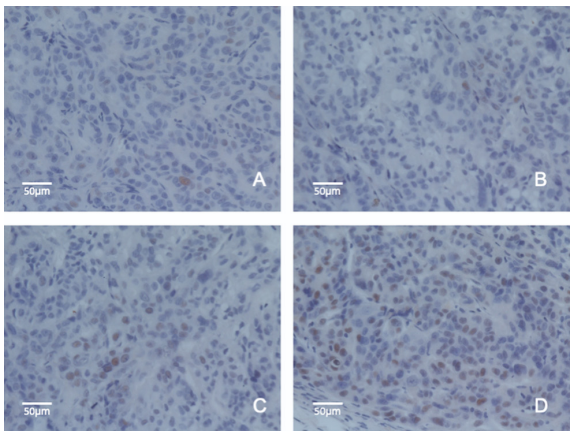

Figure 3. Tumor apoptosis after treatment in four groups (×400). (A) and **(B)** There were a few scattered apoptotic cells in the control and MBs groups. **(C)** Apoptotic cells increased and were scattered in the US group. **(D)** Apoptotic cells significantly increased and were present in sheets in the US + MBs group.

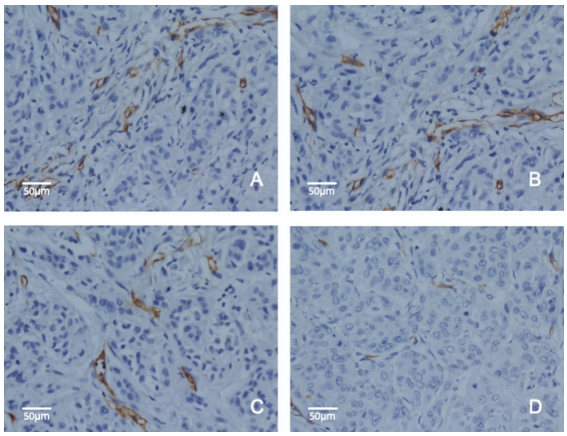

Figure 4. MVD after treatment in four groups (×400). (A) and **(B)** There are many microvessels in the control and MBs group. **(C)** Microvessels decreased slightly in the US group. **(D)** Microvessels decreased significantly in the US + MBs group, and the residual lumens are mostly closed. MVD: microvascular density.

mostly closed. MVD in the US group was lower than that in the control and MBs groups ($p < 0.001$). The MVD in the US + MBs group (3.75 ± 0.36) was markedly lower than that in the other three groups (US: 11.04 ± 0.34; MBs: 6.15 ± 0.29; and control: 4.68 ± 0.22; $p < 0.001$ for all). There were no significant differences in the MVD in the control and MBs groups ($p > 0.05$). The MVDs in the four groups are shown in Table 2.

Discussion

US is widely investigated and has developed in diagnostic and therapeutic fields, and low-frequency US is currently a topic of therapeutic study. Compared to high-frequency US, low-frequency US produces less heat and more cavitation. The ability of low-frequency US to inhibit tumor proliferation had been proved in several studies. Jang *et al*. observed cell death in melanoma cells mixed with Optison MBs after low-intensity US (*15*). Cao *et al*. found that low-intensity US suppressed the ability to proliferate, form colonies, and invade AsPC-1 cells (*11*). However, its clinical use in breast cancer *in vivo* is still unclear. The current study established a breast cancer model in nude mice and then subjected breast cancer xenografts to low-frequency US treatment combined with MBs. This study tried to clarify its clinical effects and discussed the underlying mechanisms.

Different US regimens can lead to different cell outcomes. When the frequency is fixed, total cell death and the ratio of necrosis increases with increasing intensity (*16*). In our previous study, we used different parameters for US (1 MHz) to treat breast cancer xenografts in nude mice. US at a frequency of 1 MHz, an intensity of 2 W/cm^2, and a duty cycle of 50% maximally inhibited tumor growth without the death of nude mice. With the current treatment, low-frequency US (a frequency of 1 MHz, an intensity of 2 W/cm^2, a duty cycle of 50%) significantly inhibited breast cancer xenografts, as evinced by the inhibition of tumor growth and abundant apoptotic cells, especially in the US + MBs group. Interestingly, there was no evidence of necrosis during the whole treatment. When tumors were treated with HIFU, significant coagulation necrosis may occur (*9,17*). The current study indicated that tumor destruction induced by low-frequency US was due to cell apoptosis, rather than cell necrosis.

When US irradiation at a specific frequency and intensity is applied to a liquid, cavitation nuclei will be created, followed by a change in volume, collapse, and a burst of the nuclei. Transient cavitation bubbles oscillate strongly and exist for only a few acoustic cycles, eventually collapsing, producing a large number of free radicals and a high local temperature and pressure (*18,19*). Oscillating bubbles also create microstreaming, which can induce shear stress on nearby cells or vessel endothelium (*20*). In addition, the force of radiation pushes bubbles towards the direction of wave propagation, which may have some impact on the endothelium. Actions on endothelium cause various stimuli, which are related to cell apoptosis alone or together, including damage to nuclear DNA (*21*), reactive oxygen species (*22*), a change in membrane permeability (*23*), disturbance of the calcium balance (*24,25*), and stimulation of the endoplasmic reticulum (*26*).

All of the above proved that cavitation-related effects lead to apoptosis. However, inducing cavitation in whole blood is not easy, probably because the body continuously filters impurities, including cavitation nuclei (*27*). SonoVue MBs were used as artificial cavitation nuclei, which markedly lowered the cavitation threshold and amplified the effect of US. Results indicated significantly better efficacy in the US + MBs group than that in the US group, which was confirmed in several other studies. Shen *et al.* used US at a frequency of 21 kHz on rabbit VX2 liver tumors, and the TGI was the highest in the US + MB group (*28*). Cao *et al.* indicated that US at a frequency of 45 kHz had the most efficient effect on decreasing cell viability and suppressing the ability of AsPC-1 cells to proliferate and form colonies in the US + MB group (*11*). However, comparing the efficacy of US across studies is not easy because different investigators used different US parameters and treatment conditions and acted on different targets.

In addition to cavitation, thermal effect is one of the essential bioeffects of low-frequency US. Mild hyperthermia can induce apoptosis in tumor cells and act synergistically with other therapies since it leads to several significant physiological changes by increasing the tumor blood flow and the perfused fraction of the tumor (*29-31*). When modulated electro-hyperthermia treatment was applied to the BALB/c mouse isograft model, the elevated expression of heat shock protein (HSP) 70 indicated heat shock-related cell stress, and the treated tumor showed significant signs of apoptosis and upregulation of caspase-3 (*32*). The stress protein response to US irradiation produced a large amount of HSPs, and elevated levels of HSP can trigger apoptosis (*32*). All of the above indicate that hyperthermia plays a certain role in oncotherapy. It has rarely been used clinically alone or with other therapies, so more research needs to be conducted in the future.

Neovascularization is associated with the reproduction, invasion, and metastasis of tumors. The destruction of supply vessels that provide sufficient oxygen and other nutrients to tumor cells can inhibit the growth of a tumor. The current study noted obvious vessel damage and erythrocyte leakage in the US + MBs group, which might be related to the cavitation and thermal effects of low-frequency US. Shock waves generated by MBs collapsing near the vessel wall may create liquid jets that damage endothelium and

cause holes in the vessel wall, activating coagulation and causing thrombosis (*33*). Shen *et al.* found that sonication with low-frequency US at 20 kHz and MBs of the rabbit carotid artery formed holes, local vascular wall defects, and arterial elastic membrane separation (*34*). Shen *et al.* indicated that diffused interstitial hemorrhages and vascular thrombi were observed after US treatment with MBs in rabbit VX2 hepatic tumors (*28*). The above studies indicated that low-frequency US combined with MBs can disrupt supply vessels, which may explain the inhibition of tumor growth.

Compared to vessels of normal tissue, tumor vessels are immature, abnormal, and highly permeable. Some large tumor vessels lack smooth muscle and are only consist of endothelium and a basement membrane. The endothelium in tumors is also structurally defective; it is discontinuous and full of gaps, causing hemorrhaging and facilitating permeability. Poorly differentiated cell contacts, abnormal cell-cell junctions, and exaggerated leakiness cause defects in endothelial cell barrier function (*35*). Tumor vessel density is very heterogeneous, and the arrangement of vessels is chaotic, especially in the center (*35*). Due to either increased endothelial permeability or tortuous vessels, the blood flow rate in tumor sites decreases, and MBs tend to be trapped at tumor sites rather than normal tissue sites. DeOre *et al*. found that the longer the residence time of MBs, the more sufficient thermal effects of damaging the endothelium (*36*). The difference in temperature enables the selective disruption of tumor blood vessels without causing a significant adverse effect on normal blood vessels (*37*).

In our study and other studies, low-frequency US has displayed a certain level of efficacy on solid tumors and no skin damage, death of mice, or metastasis were observed in our study, there are still concerns about the negative impact of using low-frequency US. For this reason, some researchers have discussed the possible negative effects of low-frequency US irradiation. Yang *et al.* found that after exposure to 0.6W/cm^2 for 15 minutes, epidermal and dermal necrosis, excoriation, and inflammatory cell infiltration were seen in skin tissue (*38*). While after exposure to 0.35W/cm^2 for 15 min, mouse skin displayed no obvious changes (*38*). Hence, at certain frequencies and intensities, US irradiation caused no significant damage to the skin of mice. Similarly, when controlled within a certain threshold, the effect of US irradiation on human skin is negligible (*39*). Although whether low-frequency US irradiation does harm to the surrounding normal tissues was not considered in our study, it has been determined by other researchers. Wang *et al.* treated mouse pancreatic cancer cells and normal pancreatic ductal epithelial cells with low-frequency US; with MB concentrations under 15%, the viability of normal pancreatic cells was not affected, while with MB concentrations under 30%, the rate of inhibition of pancreatic cancer cells increased progressively (*40*). The difference between normal cells and cancer cells when subjected to low-frequency US irradiation is closely related to apoptotic factors. For example, survivin is a member of the inhibitor of apoptosis protein family, which are selectively expressed in various malignant tumors but which are not expressed or which are expressed at lower levels in normal tissues (*41*). Under the action of low-frequency US, the up- and down-regulation of pro- and anti- apoptotic factors jointly leads to the apoptosis of cancer cells, thereby inhibiting the proliferation of cancer cells. Studies have shown that low-frequency US irradiation can inhibit the migration of cancer cells, thereby reducing the possibility of metastasis. In a study by Wei *et al*., low-frequency US was applied to prostate cancer cells, and cancer cell migration in the experimental group was significantly inhibited compared to that in the control group (*42*). In a study by Wang *et al*., low-frequency US irradiation slightly decreased the migration of pancreatic cancer cells (*40*). When cells have stem cell-like features, they were considered to be the main cause of metastasis and drug resistance (*43*). Yang *et al*. found that low-intensity US suppressed the migration of ovarian cancer stem cells by inducing morphological changes, F-actin formation, and increasing membrane stiffness (*44*). These findings indicate that under appropriate conditions, low-frequency US irradiation will not damage the skin of the experimental subject or even the patient, its effect on cancer cells and normal cells differs significantly, and it inhibits the metastasis of cancer cells to a certain degree.

There were several limitations in this study. First, this study was based on a single type of breast cancer cell, whereas there are multiple types of breast cancer cells in clinical practice. More experiments need to be designed to verify whether low-frequency US combined with MBs will still work on the other types of breast cancer. Second, this study did not explore underlying mechanisms. The continued exploration of cavitation, its molecular mechanisms, and the dose-response relationship between US parameters and anticancer efficiency need to be further studied. Third, this study only noted an inhibitory effect of low-frequency US irradiation on breast cancer cells, but the treatment failed to completely destroy cancer cells, so whether it can be used alone in clinical settings or how it can be combined with other treatments, such as chemotherapy and radiotherapy, needs to be verified further.

In conclusion, the results of this study indicated that combining low-frequency US with MBs can suppress tumor growth by inducing apoptosis and blocking the blood supply. The optimization of low-frequency US treatment should enable it to be an essential tool in the treatment of breast cancer.

Funding: This work was supported by grants from a

project for the Science and Technology Innovation Action Plan-Medical Innovation Research Program of the Shanghai Municipal Science and Technology Commission (grant no. 22Y11911600 to L Chen) and projects under the National Natural Science Foundation of China (grant no. 82374243 to L Wang and grant no. 82304906 to LS Li).

Conflict of Interest: The authors have no conflicts of interest to disclose.

References

1. Sung H, Ferlay J, Siegel RL, Laversanne M, Soerjomataram I, Jemal A, Bray F. Global cancer statistics 2020: GLOBOCAN estimates of incidence and mortality worldwide for 36 cancers in 185 countries. CA Cancer J Clin. 2021; 71:209-249.
2. Carioli G, Malvezzi M, Rodriguez T, Bertuccio P, Negri E, La Vecchia C. Trends and predictions to 2020 in breast cancer mortality in Europe. Breast. 2017; 36:89-95.
3. Zheng R, Zhang S, Zeng H, Wang S, Sun K, Chen R, Li L, Wei W, He J. Cancer incidence and mortality in China, 2016. J Natl Cancer Center. 2022; 2:1-9.
4. Loibl S, Poortmans P, Morrow M, Denkert C, Curigliano G. Breast cancer. Lancet. 2021; 397:1750-1769.
5. Waks AG, Winer EP. Breast cancer treatment: A review. JAMA. 2019; 321:288-300.
6. Bradley JA, Mendenhall NP. Novel radiotherapy techniques for breast cancer. Annu Rev Med. 2018; 69:277-288.
7. Xia LY, Hu QL, Xu WY. Efficacy and safety of radiofrequency ablation for breast cancer smaller than 2 cm: A systematic review and meta-analysis. Front Oncol. 2021; 11:651646.
8. Yu M, Pan H, Che N, *et al*. Microwave ablation of primary breast cancer inhibits metastatic progression in model mice *via* activation of natural killer cells. Cell Mol Immunol. 2021; 18:2153-2164.
9. Feril LB, Fernan RL, Tachibana K. High-intensity focused ultrasound in the treatment of breast cancer. Curr Med Chem. 2021; 28:5179-5188.
10. Peek MC, Ahmed M, Napoli A, ten Haken B, McWilliams S, Usiskin SI, Pinder SE, van Hemelrijck M, Douek M. Systematic review of high-intensity focused ultrasound ablation in the treatment of breast cancer. Br J Surg. 2015; 102:873-882; discussion 882.
11. Cao J, Hu C, Zhou H, Qiu F, Chen J, Zhang J, Huang P. Microbubble-mediated cavitation promotes apoptosis and suppresses invasion in AsPC-1 cells. Ultrasound Med Biol. 2021; 47:323-333.
12. Wu Y, Liu X, Qin Z, Hu L, Wang X. Low-frequency ultrasound enhances chemotherapy sensitivity and induces autophagy in PTX-resistant PC-3 cells *via* the endoplasmic reticulum stress-mediated PI3K/Akt/mTOR signaling pathway. Onco Targets Ther. 2018; 11:5621-5630.
13. Ji Y, Han Z, Shao L, Zhao Y. Evaluation of *in vivo* antitumor effects of low-frequency ultrasound-mediated miRNA-133a microbubble delivery in breast cancer. Cancer Med. 2016; 5:2534-2543.
14. Zhang B, Zhou H, Cheng Q, Lei L, Hu B. Low-frequency low energy ultrasound combined with microbubbles induces distinct apoptosis of A7r5 cells. Mol Med Rep. 2014; 10:3282-3288.
15. Jang KW, Seol D, Ding L, Lim TH, Frank JA, Martin JA. Ultrasound-mediated microbubble destruction suppresses melanoma tumor growth. Ultrasound Med Biol. 2018; 44:831-839.
16. Feng Y, Tian Z, Wan M. Bioeffects of low-intensity ultrasound *in vitro*: Apoptosis, protein profile alteration, and potential molecular mechanism. J Ultrasound Med. 2010; 29:963-974.
17. Guan L, Xu G. Damage effect of high-intensity focused ultrasound on breast cancer tissues and their vascularities. World J Surg Oncol. 2016; 14:153.
18. Merouani S, Hamdaoui O, Rezgui Y, Guemini M. Theoretical estimation of the temperature and pressure within collapsing acoustical bubbles. Ultrason Sonochem. 2014; 21:53-59.
19. Stricker L, Lohse D. Radical production inside an acoustically driven microbubble. Ultrason Sonochem. 2014; 21:336-345.
20. Nejad SM, Hosseini H, Akiyama H, Tachibana K. Reparable cell sonoporation in suspension: Theranostic potential of microbubble. Theranostics. 2016; 6:446-455.
21. Zuo K, Xu Q, Wang Y, Sui Y, Niu Y, Liu Z, Liu M, Liu X, Liu D, Sun W, Wang Z, Liu X, Liu J. L-ascorbic acid 2-phosphate attenuates methylmercury-induced apoptosis by inhibiting reactive oxygen species accumulation and DNA damage in human SH-SY5Y cells. Toxics. 2023; 11.
22. Fu Y, Ye Y, Zhu G, Xu Y, Sun J, Wu H, Feng F, Wen Z, Jiang S, Li Y, Zhang Q. Resveratrol induces human colorectal cancer cell apoptosis by activating the mitochondrial pathway *via* increasing reactive oxygen species. Mol Med Rep. 2021; 23.
23. Wang LY, Zheng SS. Advances in low-frequency ultrasound combined with microbubbles in targeted tumor therapy. J Zhejiang Univ Sci B. 2019; 20:291-299.
24. Tijore A, Yao M, Wang YH, Hariharan A, Nematbakhsh Y, Lee Doss B, Lim CT, Sheetz M. Selective killing of transformed cells by mechanical stretch. Biomaterials. 2021; 275:120866.
25. Romero-Garcia S, Prado-Garcia H. Mitochondrial calcium: Transport and modulation of cellular processes in homeostasis and cancer (Review). Int J Oncol. 2019; 54:1155-1167.
26. Zheng P, Chen Q, Tian X, Qian N, Chai P, Liu B, Hu J, Blackstone C, Zhu D, Teng J, Chen J. DNA damage triggers tubular endoplasmic reticulum extension to promote apoptosis by facilitating ER-mitochondria signaling. Cell Res. 2018; 28:833-854.
27. ter Haar G. Safety and bio-effects of ultrasound contrast agents. Med Biol Eng Comput. 2009; 47:893-900.
28. Shen ZY, Liu C, Wu MF, Shi HF, Zhou YF, Zhuang W, Xia GL. Spiral computed tomography evaluation of rabbit VX2 hepatic tumors treated with 20 kHz ultrasound and microbubbles. Oncol Lett. 2017; 14:3124-3130.
29. Dunne M, Regenold M, Allen C. Hyperthermia can alter tumor physiology and improve chemo- and radio-therapy efficacy. Adv Drug Deliv Rev. 2020; 163-164:98-124.
30. Liao S, Hu X, Liu Z, Lin Y, Liang R, Zhang Y, Li Q, Li Y, Liao X. Synergistic action of microwave-induced mild hyperthermia and paclitaxel in inducing apoptosis in the human breast cancer cell line MCF-7. Oncol Lett. 2019;

17:603-615.
31. Qu Y, Li J, Ren J, Leng J, Lin C, Shi D. Enhanced magnetic fluid hyperthermia by micellar magnetic nanoclusters composed of Mn(x)Zn(1-x)Fe(2)O(4) nanoparticles for induced tumor cell apoptosis. ACS Appl Mater Interfaces. 2014; 6:16867-16879.
32. Danics L, Schvarcz CA, Viana P, Vancsik T, Krenacs T, Benyo Z, Kaucsar T, Hamar P. Exhaustion of protective heat shock response induces significant tumor damage by apoptosis after modulated electro-hyperthermia treatment of triple negative breast cancer isografts in mice. Cancers (Basel). 2020; 12.
33. Chen H, Brayman AA, Kreider W, Bailey MR, Matula TJ. Observations of translation and jetting of ultrasound-activated microbubbles in mesenteric microvessels. Ultrasound Med Biol. 2011; 37:2139-2148.
34. Shen ZY, Jiang YM, Zhou YF, Si HF, Wang L. High-speed photographic observation of the sonication of a rabbit carotid artery filled with microbubbles by 20-kHz low frequency ultrasound. Ultrason Sonochem. 2018; 40:980-987.
35. Ribatti D, Nico B, Crivellato E, Vacca A. The structure of the vascular network of tumors. Cancer Lett. 2007; 248:18-23.
36. DeOre BJ, Galie PA, Sehgal CM. Fluid flow rate dictates the efficacy of low-intensity anti-vascular ultrasound therapy in a microfluidic model. Microcirculation. 2019; 26:e12576.
37. Levenback BJ, Sehgal CM, Wood AK. Modeling of thermal effects in antivascular ultrasound therapy. J Acoust Soc Am. 2012; 131:540-549.
38. Yang M, Xie S, Adhikari VP, Dong Y, Du Y, Li D. The synergistic fungicidal effect of low-frequency and low-intensity ultrasound with amphotericin B-loaded nanoparticles on C. albicans *in vitro*. Int J Pharm. 2018; 542:232-241.
39. Ahmadi F, McLoughlin IV, Chauhan S, ter-Haar G. Bio-effects and safety of low-intensity, low-frequency ultrasonic exposure. Prog Biophys Mol Biol. 2012; 108:119-138.
40. Wang H, Ding W, Shi H, Bao H, Lu Y, Jiang TA. Combination therapy with low-frequency ultrasound irradiation and radiofrequency ablation as a synergistic treatment for pancreatic cancer. Bioengineered. 2021; 12:9832-9846.
41. Westphal S, Kalthoff H. Apoptosis: Targets in pancreatic cancer. Mol Cancer. 2003; 2:6.
42. Wei C, Bai WK, Wang Y, Hu B. Combined treatment of PC-3 cells with ultrasound and microbubbles suppresses invasion and migration. Oncol Lett. 2014; 8:1372-1376.
43. Huang T, Song X, Xu D, Tiek D, Goenka A, Wu B, Sastry N, Hu B, Cheng SY. Stem cell programs in cancer initiation, progression, and therapy resistance. Theranostics. 2020; 10:8721-8743.
44. Yang Y, Du M, Yu J, Chen Z. Biomechanical response of cancer stem cells to low-intensity ultrasound. J Biomech Eng. 2023; 145.

Received June 8, 2024; Revised August 16, 2024; Accepted August 20, 2024.

Released online in J-STAGE as advance publication August 24, 2024.

[§]*These authors contributed equally to this work.*
**Address correspondence to*:
Lin Chen, Department of Ultrasound, Huadong Hospital, Fudan University, 221 West Yan'an Road Shanghai, 200040, China.
E-mail: cl_point@126.com

Ling Wang, Laboratory for Reproductive Immunology, Obstetrics and Gynecology Hospital of Fudan University, 419 Fangxie Road, 200011 Shanghai, China.
E-mail: Dr.wangling@fudan.edu.cn